

Validation of a Difussion Model Using Moisture Profiles Measured by Means of TD-NMR in Apples (*Malus domestica*)

Óscar Rodríguez · Valeria S. Eim · Susana Simal · Antoni Femenia · Carmen Rosselló

Received: 12 July 2011 / Accepted: 14 October 2011 / Published online: 30 October 2011
© Springer Science+Business Media, LLC 2011

Abstract Time domain nuclear magnetic resonance has been used to obtain experimental moisture profiles of apples during convective drying. The drying curves obtained at temperatures of 50 °C, 60 °C, 70 °C, 80 °C and 90 °C during convective drying have been modelled using a diffusion model, solved by a finite elements method. The parametric identification was carried out by comparing the experimental and simulated drying curves, and the validation of the model was conducted by comparing the experimental and the simulated moisture profiles. The proposed diffusion model including solid shrinkage and temperature influence on the diffusion coefficient allowed an adequate prediction of not only the drying curves (MRE=5.4±0.8%) but also the moisture profiles (MRE=11.0±1.7%). These results support the hypotheses admitted to formulate the mathematical equations of the model and demonstrate the usefulness of this methodology to validate the proposed model.

Keywords Time domain-NMR · Moisture profiles · Diffusion model · Apple

Nomenclature

A_r Rectangular face area (m²; Eq. 2)
 A_s Square face area (m²; Eq. 1)
 a_w Water activity (Eq. 8)
 C_0 Entropic accommodation factor (Eq. 9) dimensionless
 C_g Guggenheim constant (Eq. 8)

D_0 Pre-exponential factor (m²/s; Eq. 4)
 D_e Effective diffusion coefficient (m²/s; Eq. 3)
 e_1 Short thickness (m; Eq. 1)
 e_2 Long thickness (m; Eq. 2)
 e_2^0 Initial long thickness (m; Eq. 7)
 E_a Activation energy (J/mol; Eq. 4)
 ΔH_1 Difference between the heats of sorption of the monolayer and the multilayer of water (J/mol; Eq. 9)
 ΔH_2 Difference between the vaporisation heat of water and the sorption heat of the multilayer of water (J/mol; Eq. 10)
 K_0 Entropic accommodation factor (Eq. 10)
 K_g Constant in the GAB model (Eq. 8)
 L Half length of the parallelepiped (m)
 MRE Mean relative error (%)
 M Moisture content (kg water/kg dm)
 N Number of samples (Eq. 6)
 R Universal gas constant (J/mol K; Eq. 4)
 RH Relative humidity (%)
 $RMSE$ Root mean square error
 r^2 Correlation coefficient
 SE Standard error
 S_y Standard deviation (sample; Eq. 5)
 S_{yx} Standard deviation (estimation; Eq. 5)
 T Temperature (°C)
 t Time (s)
 V_c Calculated value (Eq. 6)
 V_e Experimental value (Eq. 6)
 var Explained variance (%)
 \bar{W} Average moisture content (kg water/kg dm)
 W_e Equilibrium moisture content (kg water/kg dm)
 W_m Monolayer moisture content (kg water/kg dm; Eq. 8)
 W_l Local moisture content (kg water/kg dm) (Eq. 3)
 x Distance (m)
 δ Nominal length dimensionless

Ó. Rodríguez · V. S. Eim · S. Simal (✉) · A. Femenia · C. Rosselló
Department of Chemistry, Universitat de les Illes Balears,
Cra. Valldemossa km 7.5,
07122 Palma de Mallorca, Spain
e-mail: susana.simal@uib.es

Introduction

In convective drying, once the air flow velocity and temperature are quite high and humidity low enough that external transfers cannot be limiting processes for the operation, water transport through a porous material as found in most solid agricultural products, is a complex phenomenon influenced by the operating conditions, characteristics of the food and thermophysical properties. Initially, the product has a certain moisture content uniformly distributed throughout its interior; once the drying process begins, a moisture profile appears as a consequence of the moisture concentration gradient between food and drying air (Dissa et al. 2008). As water is the main component of food, measurements of the water content changes during drying are therefore valuable when it comes to controlling drying processes and assuring the stability of the final product. In practice, measurement of water profiles inside biological materials is difficult because water gradients are steep and the product shrinks with water removal (Nguyen et al. 2006). Regarding the importance of the moisture distribution, various proposals for the experimental determination of moisture profiles have been suggested in the literature.

Near-infrared reflectance has been used for this purpose by authors like Wählby and Skjöldebrand (2001) and Yavari et al. (2011) to measure the change in moisture content inside small samples of pork meat and buns during a cooking process, and to monitoring the water loss of chicken nuggets during a frying process. On the other hand, magnetic resonance imaging (MRI) has been used to determine local moisture contents by Frías et al. (2002) in paddy rice, by Nguyen et al. (2006) in pears, and by Xing et al. (2007) in pasta. This technique is used due to its non-invasive and nondestructive nature. Nevertheless, MRI equipments are expensive and drying cells need to be customised and carefully designed to be adapted to the probe head of the MRI equipment.

Recently, time domain nuclear magnetic resonance (TD-NMR) has been used to quantify the water content in some agro-food products, offering a distinction between free, physically bound, and chemically bound water. In a TD-NMR experiment, the magnetic moments of the nuclei are manipulated by suitably chosen electromagnetic radio frequency fields because of this condition the method can be made sensitive to only hydrogen (^1H) and therefore to water (Rudi et al. 2008). Due to the fact of free induction decay, NMR signal amplitude is directly proportional to the quantity of liquid in the sample (Rutledge 2001; Todt et al. 2006). Then TD-NMR has been used in fresh cheese to characterise the water-holding capacity (Hinrichs et al. 2004), in biscuits to monitor the water content evolution during cooking (Assifaoui et al. 2006), in apple discs to monitor the water mobility (Sosa et al. 2010), and also

water and fat content have been simultaneously determined in caramels (Rudi et al. 2008), and in minced meat (Sørland et al. 2004) by means of this technique.

Despite that measuring local moisture contents requires to slice the sample previously, TD-NMR has the advantage of not requiring any pretreatment of the samples to be investigated, making the measurement of large amount of samples possible in short times; besides, nowadays, the laboratory space is a premium and TD-NMR devices do not take a lot of valuable laboratory bench space and its operation is of low decibel noise. Operations cost is minimum due to its low power consumption and maintenance-free ventilation concept.

Authors previously cited have been able to measure local moisture contents in different agro-food products, but have not focused their works to validate a diffusion model from the moisture profiles obtained by mean of any experimental technique mentioned. Mathematical modelling and simulation of drying curves and moisture profiles by a diffusion model has been considered to be a powerful tool to calculate and design this operation (Baini and Langrish 2007; Bon and Kudra 2007; Di Scala and Crapiste 2008).

Therefore, the objectives of this study are, on the one hand, to evaluate the usefulness of the TD-NMR in measuring the moisture distribution inside a solid during convective drying and, on the other hand, to use these moisture profiles to validate a mathematical model representative of this process.

Materials and Methods

Fresh Golden apple fruits (*Malus domestica*) were purchased in a local market, washed, peeled, cored, and cut into parallelepipedic shapes ($0.01 \times 0.01 \times 0.02$ m). The selection of apple as a raw matter was made due to not only its high worldwide production, but also because when apple is peeled and cored, is easily cut into regular homogenous and uniform solids. Some mathematical models have been proposed in the literature to simulate the drying curves of apple (Moreira et al. 2000; Kaya et al. 2007); however, those models were not validated by estimating the experimental moisture profile variation.

The total soluble solids content of apples, measured as °Brix (20 °C) was of $11.0 \pm 0.5\%$. The initial moisture content (W_0) of fresh apples, obtained by using the Official Methods of Analysis of the Association of Official Analytical Chemists (AOAC) official method (AOAC International 1990) was of 5.41 ± 0.07 kg water/kg dm. Water activity was measured by using an electric hygrometer Novasina Lab MASTER-aw (Novasina AG, Lanchen, Switzerland), in samples dried until different moisture contents, from 1.29 to 0.05 kg water/kg dm. All measurements were made by triplicate at temperatures of 10 °C, 20 °C, 30 °C and 40 °C.

The apparent dimensions were measured by triplicate in parallelepiped samples (Fig. 1) with different moisture contents ranged between 5.41 and 0.10 kg water/kg dm. The area of each face was measured by using an image acquisition system which consisted of a digital camera vertically placed above the sample at a distance of 0.3 m from its upper face. The illumination was achieved with four fluorescent light tubes (power, 35 W; length, 0.30 m; colour temperature, 2,700 K; light flux, 270 lm). Both the camera and the illumination system were placed in a wooden box whose walls were painted black to minimise the background light. Six images were acquired for each sample (four rectangular and two square faces). Image managing involved the adjustment of the pictures with Adobe PhotoShop CS® software (*magic wand* and *brush* tool) and the area measurement with an algorithm developed by using the *Image Acquisition Toolbox* of Matlab® (The Mathworks, Inc., Natick, USA). Sample edges (e_1 and e_2) were calculated according to Eqs. 1 and 2 from the average area of the rectangular (A_r) and square (A_s) faces as shown in Fig. 1, considering the solid as homogenous according to the shrinkage.

$$e_1 = \sqrt[2]{A_s} \quad (1)$$

$$e_2 = \frac{A_r}{e_1} \quad (2)$$

The methodology was tested by measuring the surface of coins of 1 and 2 Euros, due to these objects have official surface values given by *La Fábrica Nacional de Moneda y Timbre-Real Casa de la Moneda*.

Drying experiments were carried out by triplicate in a laboratory scale drier described in a previous work (Simal et al. 2005). The average characteristics of the room air were: $T=33.0\pm 1.2$ °C and $RH=42.0\pm 4.3\%$. The air flow rate was of 4 m/s, high enough to ensure that the effect of the external resistance on the drying kinetics was negligible and the internal resistance to mass transfer controlled the process. The air flowed perpendicular to the bed. A monolayer load was used. Water losses were periodically measured by weighing the basket and its content automatically.

To analyse the one-directional mass transfer process, the rectangular surfaces of all parallelepipeds were covered with an adherent waterproof film (Albal Profesional, Cofresco Ibérica, Spain) before drying, thus water loss took place only through the uncovered surfaces (square

faces). Two sets of experiments were carried out at drying temperatures of 50 °C, 60 °C, 70 °C, 80 °C and 90 °C in order to measure, on the one hand the drying curves (average moisture content vs. drying time, set 1) and on the other hand, the experimental moisture profiles (local moisture content vs. position and drying time, set 2).

With the aim of measuring the moisture profiles, samples were taken from the convective drier at different times by triplicate. Then the cover film was removed and samples were sliced perpendicularly to the mass transfer direction into six to eight slices (0.002 m thickness approximated). All cut were made applying little pressure, avoiding deforming or squeezing. Each slice was weighed, the thickness estimated from the ratio between the slice weight and whole sample weight, and its moisture content measured by using the TD-NMR technique with a spin echo method on a Bruker Minispec mq 20 Analyzer (Bruker Biosciences Española, Madrid, Spain). The operating field strength was 0.47 T, resulting in a Larmor frequency of 19.98 MHz for ^1H . Taking into account the symmetry, two equivalent profiles were obtained for each sample, one per each half of the parallelepiped.

Previous to the moisture content measurement, the instrument was calibrated with samples of known moisture content and weight. Thus, samples having different moisture content (ranged between 5.41 and 0.13 kg water/kg dm) were prepared from apples slices (thickness 0.005 m) dried at 70 °C and 4 m/s in a convective drier. After drying, samples were kept at 4 °C for 8 h for homogenization and then grounded. A fraction of grounded sample was used to determine the moisture content by using AOAC method no. 934.06 (AOAC International 1990). Other fraction was enveloped with an adherent waterproof film (avoiding water evaporation) and placed into an 18 mm glass tube for TD-NMR signal measurement. Measurements were made at 40 °C by triplicate. Moisture content and TD-NMR signal per gramme information was used to establish the calibration curve.

Mathematical Model

With the aim of establishing a methodology to analyse the mass transfer process during the apple drying, a mathematical model was proposed. Since heating usually occurs faster than the drying process, a simplifying assumption can be that the process is considered as isotherm (De Temmerman et al. 2008). Water migration from the inside of the solid towards the gas core could take place simultaneously through different mechanisms which contribute to the total mass flux. Fick's second law of diffusion combined with the microscopic mass balance, given by Eq. 3, has been considered as explaining that the water movement inside a solid takes place, basically by means of

Fig. 1 Geometric features of the parallelepiped

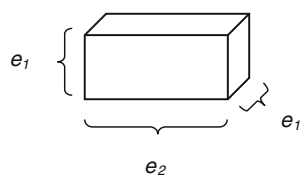
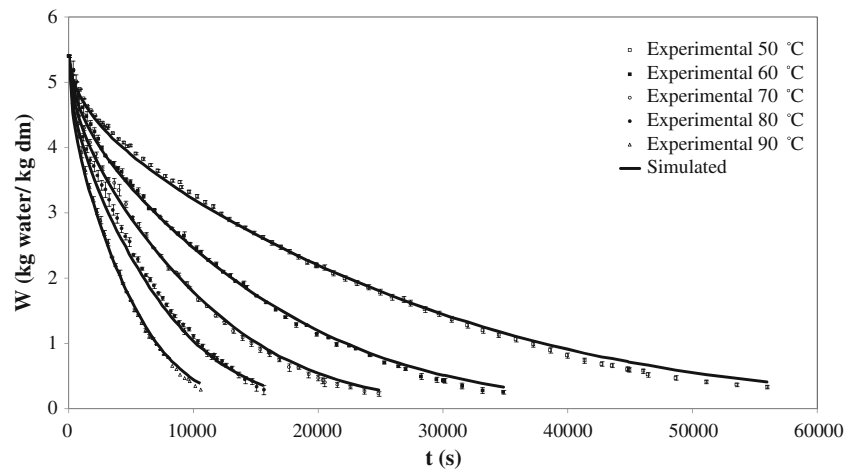


Fig. 2 Experimental and simulated drying curves of samples at different temperatures



a diffusion mechanism although other mechanisms could co-exist.

$$\frac{\partial W_l}{\partial t} = D_e \nabla^2 W_l \tag{3}$$

An effective diffusion coefficient (D_e), representative of the global transport process, might include molecular diffusion, liquid diffusion through the solid pores, vapour diffusion and all other factors which affect drying characteristics (Srikiatden and Roberts 2005; Bon and Kudra 2007). Thus, D_e was considered to be only dependent on the temperature, according to the Arrhenius relationship (Eq. 4):

$$D_e = D_0 e^{\frac{-E_a}{R(T+273.16)}} \tag{4}$$

The governing equation (Eq. 3) can be solved by assuming the following hypothesis (Simal et al. 2005; Bon and Kudra 2007): (1) the initial moisture content is uniform throughout the solid, (2) the surface of the solid is

at equilibrium with the air for the time considered, and (3) the shape and properties of the solid remain constant during the drying period considered. Thus, the boundary conditions considered can be those related to the thermodynamic equilibrium and solid symmetry. The initial condition is the initial moisture content of the sample. To finish the model formulation, sorption isotherms, psychrometric data and solid shrinkage were considered. Shrinkage was thought to be proportional in all dimensions of the solid and, according to some authors it could be related to the solid moisture content (Simal et al. 2005; Vázquez et al. 2009). In this case, when solid shrinkage is considered, the analytical solution of the differential mass transfer equation cannot be obtained, and numerical methods are needed. Thus, a finite element method was used to solve the partial differential equation. Considering a one-dimension case, the solid geometry can be divided into sub-domains perpendicularly to the mass transfer direction. COMSOL Multiphysics® (COMSOL AB) was used to solve the mathematical model, applying the finite elements method (Nguyen et al. 2006; Vázquez et al. 2009). Matlab® was used to develop the

Fig. 3 Variation of mass flux with moisture content for drying experiments carried out at temperatures of 50 °C, 60 °C, 70 °C, 80 °C and 90 °C

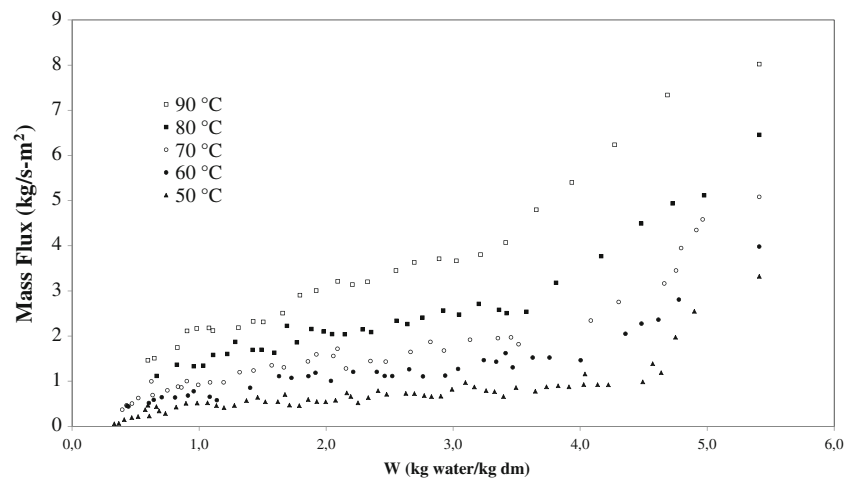
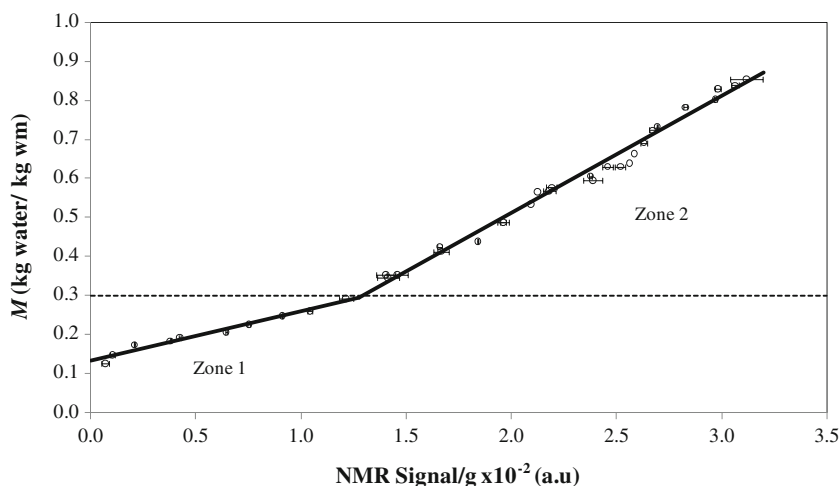


Fig. 4 Experimental moisture content (M) vs. TD-NMR signal for dried apple samples and calibration curves



algorithm to formulate and solve the optimization problem applied in the parametric identification.

Statistical Analysis and Computational Identification

In all determinations, data represent the mean and standard deviation from triplicate measurements. In this case, for solid shrinkage, drying curves and moisture profiles, the explained variance (Eq. 5) between experimental and simulated data and the mean relative error (Eq. 6) were used to assess how well the fits were. The statistic var is a measure of correlation that indicates the proportion of variability explained by the model (Kaymak-Ertekin and Gedik 2004; Souraki and Mowla 2008). S_y and S_{yx} are the total standard deviation and the standard deviation of the estimation, respectively.

$$\text{var} = \left[1 - \frac{S_{yx}}{S_y} \right] \times 100 \tag{5}$$

$$\text{MRE} = \frac{100}{N} \sum_{i=1}^N \frac{|V_e - V_c|}{V_e} \tag{6}$$

Correlation coefficient (r^2) and root mean square error (RMSE) were used to validate the TD-NMR calibration.

Table 1 TD-NMR calibration straight lines (moisture content vs. NMR signal per gramme) for the two distinct zones and their statistical parameters

Zone intervals (kg water/kg w.m)		Confidence bounds 95%	r^2	RMSE
0.12–0.30	Slope=0.127 y-Intercept=0.133	0.118, 0.136 0.127, 0.139	0.970	0.009
0.30–0.85	Slope=0.298 y-Intercept=-0.084	0.290, 0.306 -0.103, -0.065	0.987	0.019

The identification of the parameters of the equilibrium moisture isotherm model through the direct method was performed by using ‘NonLinearFit’ of the Statistic package of Mathematica 5.2 software (Wolfram Research, Inc.; Simal et al. 2007), which estimate the coefficients of a nonlinear regression function and the standard error (SE) associated to the parameters and the residuals using least squares.

In order to establish the diffusion model, the effective diffusion coefficient was identified by using the ‘fminsearch’ function of the Optimization Toolbox of Matlab® from the experimental drying curves. The sum of the mean relative errors (comparison of experimental and estimated average moisture contents at every temperature) was used as objective function to minimise (Váquiro et al. 2009).

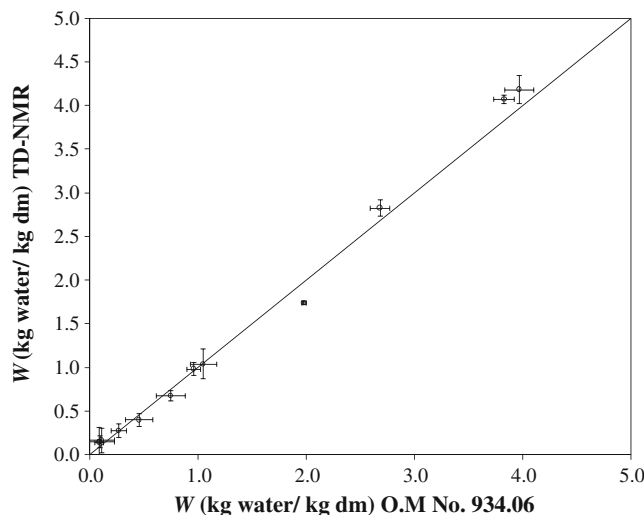
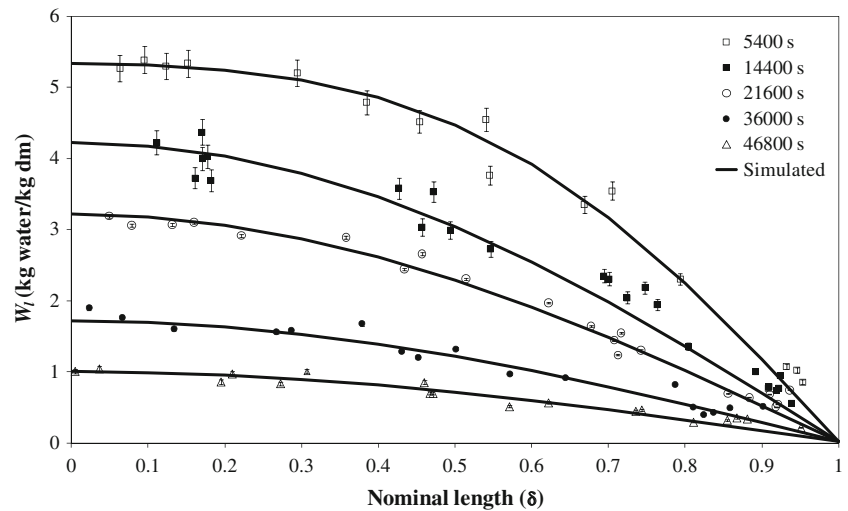


Fig. 5 Representation of the moisture content (W) measured by the TD-NMR technique and by the AOAC official method

Fig. 6 Experimental and simulated moisture profiles of apple parallelepipeds at drying temperature of 50 °C and different drying times



Results and Discussion

Solid Shrinkage

The measurements of the face areas of samples with different moisture content allowed the e_1 and e_2 determination. The apparent volume shrank by about 62% (for a moisture content ranged between 5.41 and 0.20 kg water/kg dm) of the initial volume. It was observed that, e_1 and e_2 shrinkage varied linearly with the average moisture content. However, no significant differences in the solid shrinkage behaviour among samples dried at different temperatures were observed. These results agree with the research of Bains and Langrish (2007) with bananas at drying temperatures of 60–80 °C; of Dissa et al. (2008) with mango at drying temperatures of 50 °C, 60 °C and 70 °C; and of Márquez and De Michelis (2011) with sweet and sour cherries at drying temperatures of 50 °C, 55 °C, 60 °C, 65 °C, 70 °C and 75 °C. For that reason, all data were used together, regardless

the drying temperature, to obtain a relationship between the sample thickness along the mass transfer direction and the average moisture content. The relationship obtained (Eq. 7) was used to take into account the sample shrinkage and therefore the nominal length reduction in the diffusion model and agrees with the model reported by Moreira et al. (2000) for apples disc dried during convective drying. The var and MRE obtained were of 96.4% and 2.0%, respectively.

$$\frac{e_2}{e_2^0} = (5.62 \times 10^{-2} W + 0.709) \quad r^2 = 0.965 \quad (7)$$

Drying Curves

Apple-drying curves were studied at different air drying temperatures: 50 °C, 60 °C, 70 °C, 80 °C and 90 °C for average moisture content from 5.41 to 0.2 kg water/kg dm. Figure 2 shows the experimental results and the

Fig. 7 Experimental and simulated moisture profiles of apple parallelepipeds at drying temperature of 70 °C and different drying times

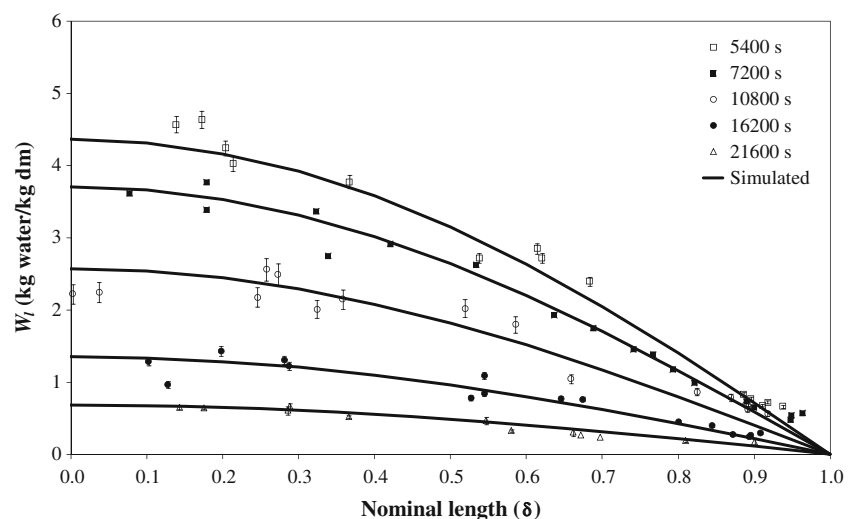
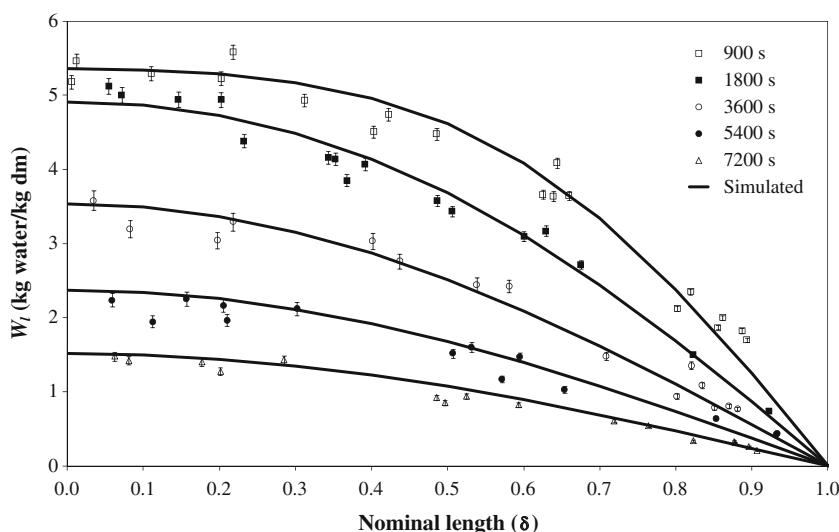


Fig. 8 Experimental and simulated moisture profiles of apple parallelepipeds at drying temperature of 90 °C and different drying times



standard deviations obtained in the measurement of the drying curves of apples (dots) corresponding to set 1. From these figures, the mass flux (mass per unit of area and time) was calculated to find out any constant mass flux stage for the drying conditions used. Considering that the solid shrinkage (Eq. 7) leads to a reduction of the exchange surface area, neither induction nor constant mass flux were observed, being the falling mass flux stage the most representative of the process (Fig. 3). As was expected, increasing the drying air temperature affected the drying curves reducing the final drying time (Dissa et al. 2008).

TD-NMR Calibration

As was mentioned above, to establish a calibration curve, the TD-NMR signal was measured in samples of different moisture contents. According to the literature, usually the TD-NMR signal varies linearly with the moisture content expressed in wet basis. Some examples have been reported by Assifaoui et al. (2006) for biscuits, whose moisture contents ranged between 0.19 and 0.32 kg water/kg dm and by Budiman et al. (2002) for cheese, whose moisture contents ranged between 0.43 and 0.54 kg water/kg dm. However, in this study, the determination of moisture

profiles requires a calibration curve including a wider moisture content range.

Experimental results of moisture content expressed as kilogramme water per kilogramme wet mass (wm) vs. TD-NMR signal per gramme and their standard deviations are represented in Fig. 4. It is known that the TD-NMR signal is not only the consequence of the water content but also of the water-binding properties (Rutledge 2001). In this figure, two zones can be observed in which the moisture content varies linearly with the TD-NMR signal with different slope in each zone. Thus, the results were fitted to two straight lines, one for each zone, by using the *Curve Fitting Toolbox* of Matlab®. These fits were also represented in Fig. 4. The slope, the y-intercept and the statistical parameter of the two straight lines are summarised in Table 1.

Table 2 Parameter values of the GAB model and the standard error associated

Parameter	Estimated	SE
Wm(% dm)	12.01	0.39
C ₀	0.047	0.007
ΔH ₁ (J/mol)	8842.61	390.58
K ₀	1.09	0.03
ΔH ₂ (J/mol)	-296.72	69.33

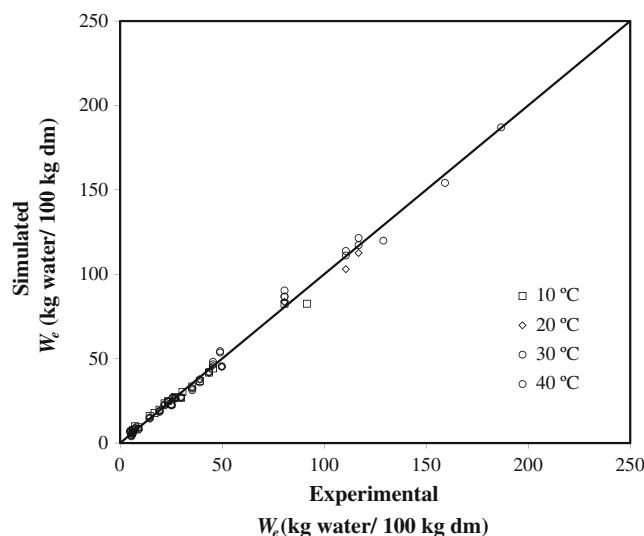


Fig. 9 Simulated vs. experimental equilibrium moisture content. Experiments carried out at temperatures of 10 °C, 20 °C, 30 °C and 40 °C

To validate the calibration, the moisture content of samples not used in the calibration was predicted and compared with that obtained using the official AOAC method (AOAC International 1990). The comparison and the standard deviations are shown in Fig. 5. A good correlation between both groups of data can be observed ($r^2=0.992$); the y -intercept was found to be significantly equal to zero ($p<0.05$) and the slope figure was of 1.02 ± 0.06 . The obtained RMSE of 0.02 kg water/kg wm was satisfactory. According to the results, the proposed TD-NMR calibration could be considered suitable to accurately determine the moisture content of apple samples.

Moisture Profiles

The moisture distribution as a function of both position and drying time was determined (experiments of set 2). As examples, Figs. 6, 7 and 8 show the experimental moisture profiles and the standard deviations (dots) obtained at the drying air temperatures of 50 °C, 70 °C, and 90 °C, respectively, at different drying times versus the nominal length ($\delta=x/e_2$), where 0 and 1 in the horizontal axis correspond to the centre and the centre of a square face of the parallelepiped.

The shown profiles allow to notice that the moisture content at the surface of the sample ($\delta=1$) was very low from the earliest stages of the process, this being indicative of the probable moisture equilibrium between the solid surface and the drying air; additionally, a considerable moisture gradient inside the solid can be observed. These observations could indicate that the external resistance is practically negligible, and the mass flux is mainly controlled by the internal resistance to mass transfer (Simal et al. 2005; Srikiatden and Roberts 2005).

Diffusion Model

Experimental data of water activity were used to establish a sorption isotherm according to the Guggenheim–Andersen–de Boer model (Eq. 8; Kaymak-Ertekin and Gedik 2004; Simal et al. 2007).

$$W_e = \frac{W_m C_g K_g a_w}{(1 - K_g a_w) [1 + (C_g - 1) K_g a_w]} \tag{8}$$

The statistical analysis of the non-linear regression demonstrated that the influence of the temperature on the monolayer moisture content (W_m) within the studied temperature range (10–40 °C) was negligible. This fact agrees with the results of other authors carried out in similar studies with grapes, apricots, apples, potatoes and red pepper (Kaymak-Ertekin and Gedik 2004; Di Scala and Crapiste 2008). Therefore, the influence of the temperature

Table 3 Identified figures for D_e , var, and MRE obtained by comparison between the experimental and simulated drying curves at different temperatures

Temperature (°C)	$D_e \times 10^9$ (m ² /s)	var (%)	MRE (%)
50	1.15±0.08	99.7±0.3	4.3±0.4
60	1.96±0.01	99.7±0.1	4.4±0.5
70	2.86±0.02	99.7±0.5	5.9±0.7
80	4.01±0.05	99.4±0.4	6.1±0.8
90	6.11±0.02	99.4±0.4	6.2±0.5
Average		99.6±0.1	5.4±0.8

was considered only in C_g and K_g parameters, according to Eqs. 9 and 10. Thus, five parameters were simultaneously identified ($C_0, \Delta H_1, K_0, \Delta H_2, W_m$) from experimental data, using “NonLinearFit” of the Statistic package of Mathematica 5.2 software (Wolfram Research, Inc.).

$$C_g = C_0 e^{\frac{\Delta H_1}{R(T+273.16)}} \tag{9}$$

$$K_g = K_0 e^{\frac{\Delta H_2}{R(T+273.16)}} \tag{10}$$

The result of the parametric identification and the SE associated with each parameter are shown in Table 2. Similar figures were reported by Kaymak-Ertekin and Gedik (2004) for apples. Equations 8, 9 and 10 were used together to simulate the moisture content for different water activity figures and temperatures, and compared with the experimental ones. The var and MRE obtained through this comparison were of 99.4% and 8.5%, respectively. Figure 9 shows the representation of the simulated vs. experimental equilibrium

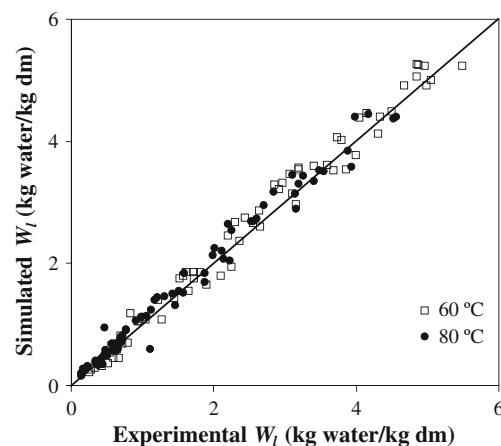


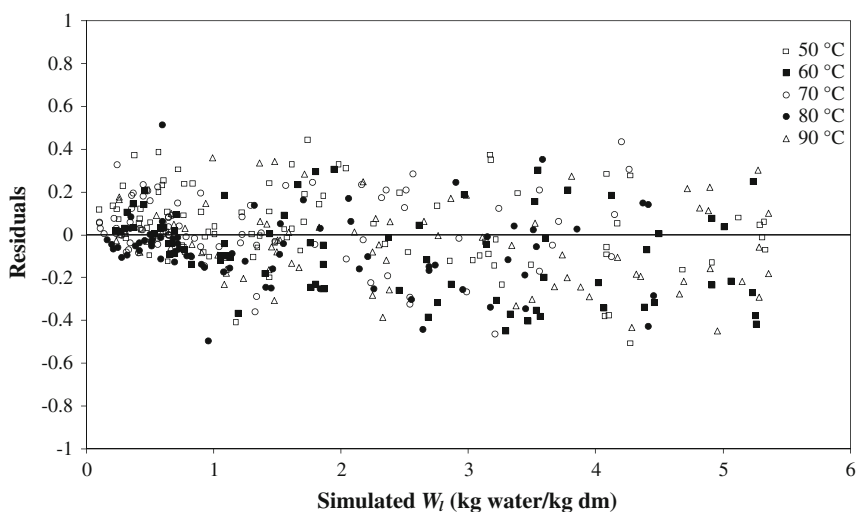
Fig. 10 Simulated vs. experimental local moisture content. Experiments carried out at temperatures of 60 °C and 80 °C

moistures content (kg water/100 kg dm) for experiments carried out at temperatures of 10 °C, 20 °C, 30 °C and 40 °C. From these results, it could be concluded that the GAB model could be appropriate to represent the water desorption of apple from 10 °C to 40 °C. This sorption isotherm was used to estimate the equilibrium moisture content (W_e) for one of the boundary conditions in the model solving. These figures were confirmed with the ones obtained by extending the drying time until no measurable weight loss was observed and ranged from 2.38×10^{-2} kg water/kg dm at 50 °C to 8.63×10^{-4} kg water/kg dm at 90 °C.

The diffusion model was designed for a one-dimensional system whose nominal length shrinks as a function of the average moisture content (Eq. 7). In order to establish the diffusion model, the effective diffusivity coefficient was identified from the experimental drying curves of apple obtained for different temperatures. The identified D_e figures, shown in Table 3, varied from $1.15 \times 10^{-9} \pm 0.08 \times 10^{-9}$ m²/s at 50 °C to $6.11 \times 10^{-9} \pm 0.02 \times 10^{-9}$ m²/s at 90 °C. Similar figures for red delicious apple have been previously reported by Srikiatden and Roberts (2005), 1.62×10^{-9} m²/s at 50 °C and 2.28×10^{-9} m²/s at 70 °C, and by Kaya et al. (2007), 1.27×10^{-10} m²/s at 35 °C and 2.02×10^{-10} m²/s at 55 °C. Although it has been reported that the effective diffusion coefficient is a function of the local moisture content (Simal et al. 2006; De Temmerman et al. 2008; Vázquez et al. 2009), the authors found a good fit by assuming that the effective diffusion coefficient is only dependent on the temperature. Equation 11 was obtained by fitting the effective diffusion coefficients identified at the different temperatures to the Arrhenius equation.

$$D_e = 2.934 \times 10^{-3} \exp \left[\frac{-39491.31}{R(T + 273.16)} \right] \quad r^2 = 0.999 \quad (11)$$

Fig. 11 Representation of the residuals vs. the simulated local moisture figures for experiments carried out at temperatures of 50 °C, 60 °C, 70 °C, 80 °C and 90 °C



The activation energy (E_a) for diffusion was of 39.5 kJ/mol. Figures for this property reported in the literature include: 58.5 in kJ/mol in peas by Senadeera et al. (2003), 27.0 kJ/mol in kiwi by Simal et al. (2005), and 47.3 kJ/mol in green beans by Souraki and Mowla (2008), among others.

Simulation of Drying Curves and Moisture Profiles

By using the proposed model together with Eqs. 3, 4, 7, 8, 9, 10, and 11, the drying curves of apple at different temperatures were simulated. The simulation is shown in Fig. 2 by the solid lines. It can be observed in this figure that the proposed model allowed an adequate simulation of these drying curves in the whole range of temperatures. To mathematically evaluate the drying curves simulation, the var and MRE were calculated and also included in Table 3. Thus it could be concluded that using the proposed model, the drying curves of apple can be satisfactorily simulated.

Furthermore, the proposed diffusion model also allows the estimation of the local moisture content variation with the drying time inside the solid. Thus, in order to better validate the model, the moisture profiles were simulated at the same drying times and temperatures of those experimentally measured. These profiles were not used in the parametric identification although they correspond to the same drying temperatures of the drying curves used to identify the D_e . Both experimental (dots) and simulated (lines) have been represented together in Figs. 6, 7 and 8 for the experiments carried out at 50 °C, 70 °C, and 90 °C. A satisfactory concordance between both experimental and simulated groups of data can be observed. Similarly, Fig. 10 shows the representation of the simulated vs. experimental local moisture content for experiments carried out at temperatures of 60 °C and 80 °C. It can

be observed how the dots are located close to the diagonal, demonstrating the high concordance between both groups of data. The simulation was mathematically evaluated by using var and MRE obtained by comparing the experimental local moisture and those given by the model for the whole range of temperatures studied. A satisfactory concordance was observed between both groups of data ($\text{var}=95.2\pm 0.8\%$ and $\text{MRE}=11.0\pm 1.7\%$). In order to better evaluate how well the model fits, Fig. 11 shows the representation of the residual vs. the simulated local moisture content for the experiments carried out at the temperatures mentioned above. It could be observed that the residuals appeared randomly scattered close around zero (from -0.5 to 0.5).

Thus, the proposed diffusion model including solid shrinkage and temperature influence on the diffusion coefficient allowed an adequate prediction not only of the drying curves but also of the moisture profiles of Golden apple samples subjected to convective drying in the temperature range from $50\text{ }^{\circ}\text{C}$ up to $90\text{ }^{\circ}\text{C}$, which supports the hypothesis admitted to formulate the mathematical equations of the model.

Conclusions

The usefulness of the TD-NMR as a technique to measure the moisture distribution as a function of the drying time inside apple samples under convective drying in the range of $50\text{ }^{\circ}\text{C}$ to $90\text{ }^{\circ}\text{C}$ has been demonstrated. The observed shape of the moisture profiles helps to better understand how the mass transport takes place during convective drying.

Moreover, this information has been used to validate a mathematical model representative of this diffusion process. The parametric identification was carried out by comparing average moisture contents (experimental and simulated) and validation of the model was conducted by comparing the experimental and the simulated moisture profiles. The proposed diffusion model including solid shrinkage and temperature influence on the diffusion coefficient allowed an adequate prediction of not only the drying curves ($\text{MRE}=5.4\pm 0.8\%$) but also the moisture profiles ($\text{MRE}=11.0\pm 1.7\%$). This methodology can be considered as an important contribution due to the fact that usually models are only validated using experimental measurements of average moisture content in the range studied.

Acknowledgements The authors would like to acknowledge the financial support from the MICINN (DPI2009-14549-C04-02) and the Research Fellowship of the Conselleria d'Innovació, Interior i Justícia (Govern de les Illes Balears).

References

- AOAC International. (1990). *Official methods of analysis of the Association of Official Analytical Chemists International*. Arginton, USA: William Horwitz.
- Assifaoui, A., Champion, D., Chiotelli, E., & Verel, A. (2006). Characterization of water mobility in biscuit dough using a low-field 1H NMR technique. *Carbohydrate Polymers*, *64*(2), 197–204.
- Baini, R., & Langrish, T. A. G. (2007). Choosing an appropriate drying model for intermittent and continuous drying of bananas. *Journal of Food Engineering*, *79*(1), 330–343.
- Bon, J., & Kudra, T. (2007). Enthalpy-driven optimization of intermittent drying. *Drying Technology: An International Journal*, *25*(4), 523.
- Budiman, E., Strohshine, R., & Cornillon, P. (2002). Moisture measurement in cheese analogue using stretched and multi-exponential models of the magnetic resonance. *The Journal of Dairy Research*, *69*, 619–632.
- De Temmerman, J., Verboven, P., Delcour, J. A., Nicolai, B., & Ramon, H. (2008). Drying model for cylindrical pasta shapes using desorption isotherms. *Journal of Food Engineering*, *86*(3), 414–421.
- Di Scala, K., & Crapiste, G. (2008). Drying kinetics and quality changes during drying of red pepper. *LWT- Food Science and Technology*, *41*(5), 789–795.
- Dissa, A. O., Desmorieux, H., Bathiebo, J., & Kouliadiati, J. (2008). Convective drying characteristics of amélie mango (*Mangifera indica* L. cv. 'Amélie') with correction for shrinkage. *Journal of Food Engineering*, *88*(4), 429–437.
- Frias, J. M., Foucat, L., Bimbenet, J. J., & Bonazzi, C. (2002). Modeling of moisture profiles in paddy rice during drying mapped with magnetic resonance imaging. *Chemical Engineering Journal*, *86*(1–2), 173–178.
- Hinrichs, R., Götz, J., Noll, M., Wolfschoon, A., Eibel, H., & Weisser, H. (2004). Characterisation of the water-holding capacity of fresh cheese samples by means of low resolution nuclear magnetic resonance. *Food Research International*, *37*(7), 667–676.
- Kaya, A., Aydın, O., & Demirtaş, C. (2007). Drying kinetics of red delicious apple. *Biosystems Engineering*, *96*(4), 517–524.
- Kaymak-Ertekin, F., & Gedik, A. (2004). Sorption isotherms and isosteric heat of sorption for grapes, apricots, apples and potatoes. *Lebensmittel-Wissenschaft Und-Technologie*, *37*(4), 429–438.
- Márquez, & De Michelis, A. (2011). Comparison of drying kinetics for small fruits with and without particle shrinkage considerations. *Food and Bioprocess Technology*, *4*(7), 1212–1218.
- Moreira, R., Figueredo, A., & Mulet, A. (2000). Shrinkage of apple disks during drying by warm air convection and freeze drying. *Drying Technology*, *18*(1&2), 279–294.
- Nguyen, T., Dresselaers, T., Verboven, P., D'hallewin, G., Culeddu, N., Van Hecke, P., et al. (2006). Finite element modelling and MRI validation of 3D transient water profiles in pears during postharvest storage. *Journal of the Science of Food and Agriculture*, *86*(5), 745–756.
- Rudi, T., Guthausen, G., Burk, W., Reh, C. T., & Isengard, H. (2008). Simultaneous determination of fat and water content in caramel using time domain NMR. *Food Chemistry*, *106*(4), 1375–1378.
- Rutledge, D. N. (2001). Characterisation of water in agro-food products by time domain-NMR. *Food Control*, *12*(7), 437–445.
- Senadeera, W., Bhandari, B. R., Young, G., & Wijesinghe, B. (2003). Influence of shapes of selected vegetable materials on drying kinetics during fluidized bed drying. *Journal of Food Engineering*, *58*(3), 277–283.
- Simal, S., Femenia, A., Garau, M. C., & Rosselló, C. (2005). Use of exponential, page's and diffusional models to simulate the drying

- kinetics of kiwi fruit. *Journal of Food Engineering*, 66(3), 323–328.
- Simal, S., Garau, M. C., Femenia, A., & Rosselló, C. (2006). A diffusional model with a moisture-dependent diffusion coefficient. *Drying Technology*, 24(11), 1365–1372.
- Simal, S., Femenia, A., Castell-Palou, Á., & Rosselló, C. (2007). Water desorption thermodynamic properties of pineapple. *Journal of Food Engineering*, 80(4), 1293–1301.
- Sørland, G. H., Larsen, P. M., Lundby, F., Rudi, A., & Guiheneuf, T. (2004). Determination of total fat and moisture content in meat using low field NMR. *Meat Science*, 66(3), 543–550.
- Sosa, N., Salvatori, D., & Schebor, C. (2010). Physico-chemical and mechanical properties of apple disks subjected to osmotic dehydration and different drying methods. *Food and Bioprocess Technology*. doi:10.1007/s11947-010-0468-4.
- Souraki, B. A., & Mowla, D. (2008). Axial and radial moisture diffusivity in cylindrical fresh green beans in a fluidized bed dryer with energy carrier: modeling with and without shrinkage. *Journal of Food Engineering*, 88(1), 9–19.
- Srikiatden, J., & Roberts, J. S. (2005). Moisture loss kinetics of apple during convective hot air and isothermal drying. *International Journal of Food Properties*, 8(3), 493.
- Todt, H., Guthausen, G., Burk, W., Schmalbein, D., & Kamlowksi, A. (2006). Water/moisture and fat analysis by time-domain NMR. *Food Chemistry*, 96(3), 436–440.
- Váquiro, H. A., Clemente, G., García-Pérez, J. V., Mulet, A., & Bon, J. (2009). Enthalpy-driven optimization of intermittent drying of *Mangifera indica* L. *Chemical Engineering Research and Design*, 87(7), 885–898.
- Wählby, U., & Skjöldebrand, C. (2001). NIR-measurements of moisture changes in foods. *Journal of Food Engineering*, 47(4), 303–312.
- Xing, H., Takhar, P. S., Helms, G., & He, B. (2007). NMR imaging of continuous and intermittent drying of pasta. *Journal of Food Engineering*, 78(1), 61–68.
- Yavari, A., Heshmati, A., Hamed, M., & Haghbin, S. (2011). VIS/NIR hyper-spectroscopy technique for the measurement of moisture and fat contents of breaded-fried chicken nuggets. *Food Chemistry*, 127(2), 645–650.